CHIN.PHYS.LETT. Vol. 25, No. 1 (2008) 234

Strong Surface Diffusion Mediated Glancing-Angle Deposition: Growth, Recrystallization and Reorientation of Tin Nanorods

WANG Huan-Hua(王焕华)[1*], SHI Yi-Jian(石益坚)[2], William CHU[2], Yigal BLUM[2]

[1]*Institute of High Energy Physics, Chinese Academy of Sciences, Beijing 100049*
[2]*SRI International, Menlo Park, CA 94025, USA*

(Received 27 August 2007)

Different from usual glancing-angle deposition where low surface diffusion is necessary to form nanorods, strong surface diffusion mediated glancing-angle deposition is exemplified by growing tin nanorod films on both silicon and glass substrates simultaneously via thermal evaporation. During growth, the nanorods were simultaneously baked by the high-temperature evaporator, and therefore re-crystallized into single crystals in consequence of strong surface diffusion. The monocrystalline tin nanorods have a preferred orientation perpendicular to the substrate surface, which is quite different from the usual uniformly oblique nanorods without recrystallization.

PACS: 64.70.Nd, 81.15.Kk, 81.07.−b, 81.40.Gh

New useful properties of thin films superior to bulk can be realized by controlling fine structures of thin films through self-assembly-based nanotechnologies, such as hydrophobic surface of nano-columnar films,[1] and radial PN junction nanorod solar cells.[2] For industrial applications, however, the self-assembly nanotechnology is required to be high-yield, low-cost, simple in procedures, suitable for large-scale production, no high vacuum needed and no material limit. Glancing angle deposition (GLAD) is such a technique that meets all these requirements.

GLAD is a unique and versatile self-assembly technique for fabricating three-dimensional nanostructured thin films.[3,4] It is a physical vapour deposition process where the deposition flux is incident on a substrate with a large incident angle with respect to the normal of the substrate surface. The flux species land on the substrate, nucleate and form randomly distributed nucleus, which leave shadowed areas where the subsequent flux cannot reach. If the substrate temperature is low enough to limit the diffusion length within several atomic distances,[5] the flux species cannot diffuse into the shadowed areas. Thus, only exposed areas receive flux and grow up into nanorods, and the shadowed areas are left vacant. By positioning the substrate during the growth, various nano-columnar structures of different shapes can be fabricated.[3−7]

A disadvantage of this technique is that the as-grown nanorods are usually amorphous. For applications that need crystalline nanorods, post-growth annealing is usually a necessary step to recrystallize GLAD nanorods.[8−11] In this study, we attempt a new route to achieve crystalline nanorods. The main idea is to grow separated nanorods at low temperatures at the initial growth stage, then to increase the temperature to crystallize the nanorod tips and generate 'crystal seeds' while growth is ongoing. The monocrystalline nanorods may continue to grow at high temperature because the newly arriving flux particles landing on the top parts of the nanorods would diffuse across the high surface energy planes of the crystalline nanorods to the low surface energy planes due to the free energy minimization. To check this idea, tin was selected for experiments. We find that the recrystallization of tin nanorods occurs during growth, and single-crystal tin nanorods are achieved without post-growth annealing needed.

Tin nano-columnar thin films were grown both on silicon (001) wafer and on glass simultaneously using a simple thermal evaporation system under glancing angle deposition configuration. Carefully cleaned silicon and glass substrates were clamped onto a holder with adjustable incident angle. Tin granules were placed into a tungsten evaporator underneath as the source. The distance between the source and the centre of the substrate is 254 mm. A background pressure of 1.5×10^{-6} Torr was generated in the growth chamber prior to the evaporation. Tin was evaporated and deposited onto the static substrates with a large incident angle. The substrates were set at room temperature at the initial growth stage, while were baked by the evaporator during evaporation. Depending upon the baking time, the sample can be baked at different high temperatures near 200°C, which can re-crystallize the tin nanorods because tin nanorods have a melting point lower than that of bulk tin metal (231.9°C). The pressure temporarily increased to no higher than 6.0×10^{-6} Torr as evaporation started, and then slowly decreased again. Anyway, the mean free path during the growth is no less than 13 m (suppose that the average radius of background gas molecules is 1.46 Å), which is much larger than the source-to-substrate distance. The growth rate can be adjusted by tuning the

* To whom correspondence should be addressed. Email: wanghh@ihep.ac.cn
© 2008 Chinese Physical Society and IOP Publishing Ltd

evaporator power.

The normal-angle deposition rate and the corresponding film thickness were measured using two Rate/Thickness Monitors (by Sycon Instrument, Inc.) that were mounted close to the substrates with a normal-angle deposition configuration. The average normal-angle deposition film thickness is recorded as monitor thickness in Table 1, versus GLAD film thickness that was measured using a JOEL JSM-6700 scanning electron microscopy (SEM). The growth rates in all the growths were increased from 0 Å/s at the beginning to 1.6 Å/s at the steady growth stage. Table 1 lists the incident angles, the growth/baking time, the monitor thickness and the film thickness of several samples.

Table 1. Samples of tin and copper nanorods.

Sample	Incident angle	Growth/baking time (min)	Monitor thickness (Å)	Film thickness (Å)
Sn-A	$\alpha = 85°$	147.5	11216	∼68800
Sn-B	$\alpha = 86°$	85.0	1549	∼520
Sn-C	$\alpha = 86°$	16.5	1026	∼350
Cu	$\alpha = 86°$	69.5	5179	∼1500

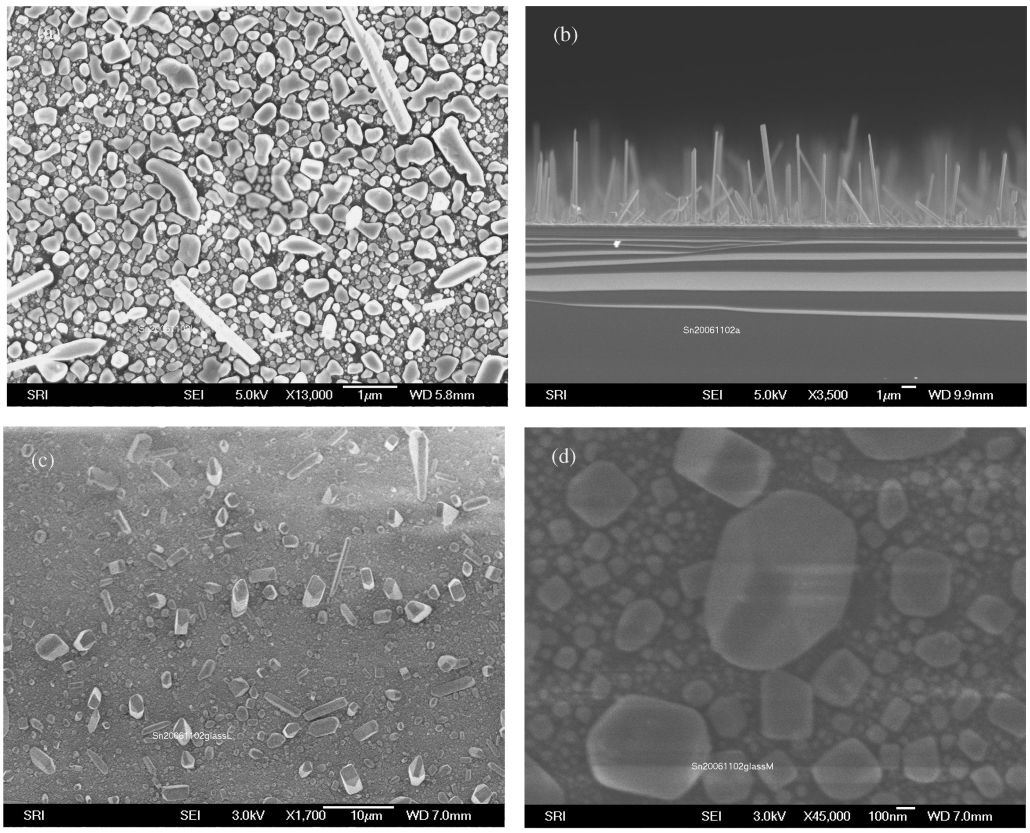


Fig. 1. Top-view (a) and cross-sectional (b) SEM images of tin nanorods on silicon wafer, and top-view SEM images [(c) and (d)] of tin nanorods on glass.

After growth, the samples were taken out for other characterizations. They were cleaved and measured using SEM. Their crystallography was characterized using x-ray diffraction (XRD) at Beijing Synchrotron Radiation Laboratory, Institute of High Energy Physics, Chinese Academy of Sciences. The monocrystallinity of the nanorods was confirmed using a Joel JEM-2010 transmission electron microscope (TEM) operating at 200 kV.

Figure 1 presents the SEM images of two tin nanocolumnar films (sample Sn-A) grown on silicon wafer and on glass at the same time. Figures 1(a) and 1(b) are the top-view and cross-section images of the tin film grown on silicon wafer. Figures 1(c) and 1(d) are the top-view images of the tin film grown on glass. It is obvious that most of the tin nanorods have regular shape, indicating that they are single crystals. They have a preferred orientation along the surface normal, around which their orientations distribute in a large angle range. It can be seen that some much longer

nanorods sporadically distribute in the forest of tin nanorods of common length, which are, in our opinion, resulted from the merging of neighbouring nanorods that are in contact with each other.

Figure 2 shows the XRD patterns of sample Sn-A shown in Figs. 1(a) and 1(b). Figure 2(a) shows the 2θ-scan results where the diffraction peaks of the silicon wafer were avoided by fixing θ at 5.35° and at 14.95°, respectively. It can be seen that two peaks (200) and (101) of tetragonal tin crystal appear at $2\theta = 30.80°$ and at $2\theta = 32.18°$, respectively. The (200) peak is much wider at $\theta = 5.35°$ than that at $\theta = 14.95°$, because the length of x-ray path in tin nanorods in the former case is shorter than that in the latter case owing to the preferred orientation of tin nanorods. Figure 2(b) is the θ-scan (rocking curve) of the tin (200) peak. We can see that θ has a large range (FWHM = 5.79°) around the peak at $\theta = 15.59°$ (about $2\theta/2$), indicating the orientation of tin nanorods distributed in a large range around the surface normal. Here θ–2θ scan was performed based on the start point $2\theta = 30.80°$ and $\theta = 14.95°$, which was deviated from the exact half of 2θ in order to avoid the peaks of silicon. The θ–2θ scan curve is shown in Fig. 2(c), three sets of peaks appearing there, which together with the SEM images shows that the film is composed of single crystals of different orientations. Figure 2(d) is the ϕ-scan curve at the (200) peak, indicating that the orientation distribution of tin nanorods is isotropic around the substrate surface normal.

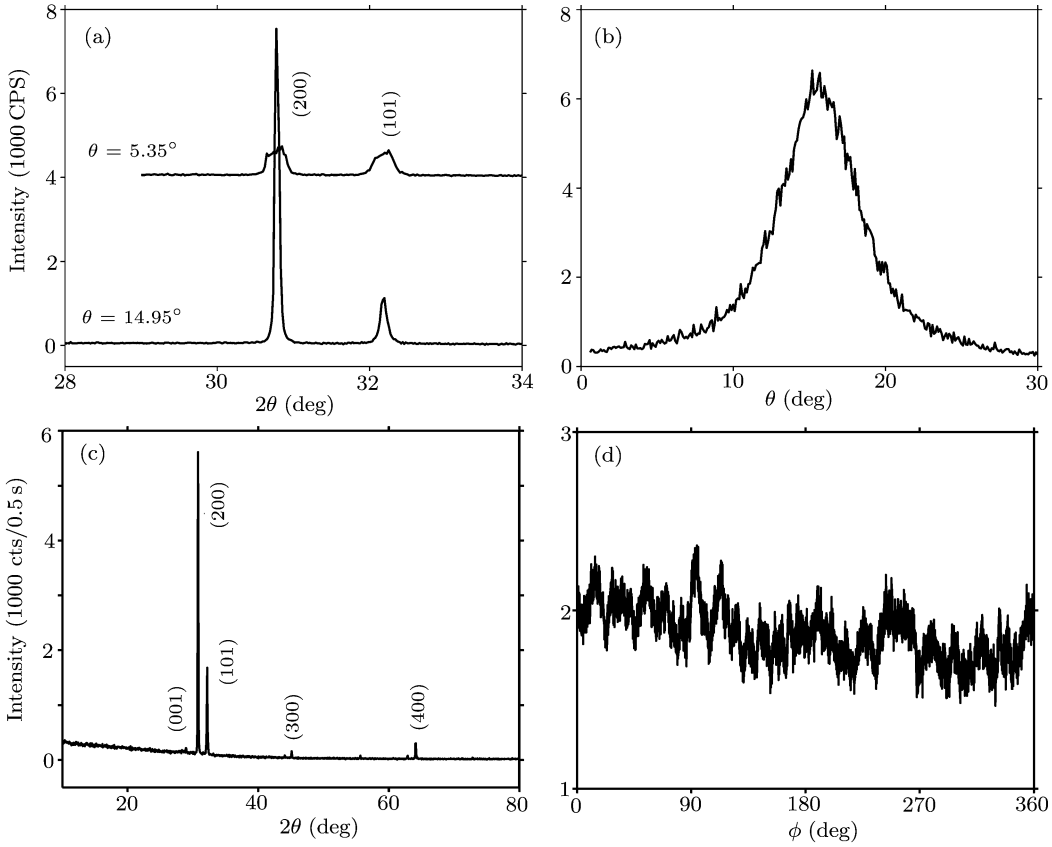


Fig. 2. XRD patterns of tin nanorods grown on silicon wafer: (a) 2θ-scan curves with fixed $\theta = 5.35°$ (upper) and at $\theta = 14.95°$ (lower), respectively; (b) θ-scan curve with 2θ fixed at the (200) peak; (c) $\theta - 2\theta$ scan curve; and (d) ϕ-scan with 2θ fixed at the (200) peak.

TEM measurements further confirm that the as-grown tin nanorods are single crystals with clear atomic layers and sharp diffraction patterns. Both the electron diffraction patterns and the real-space images are in agreement with tin crystal. The TEM results of sample A were used as an example again, as shown in Fig. 3. However, this sample had been heated in atmosphere using an electric heating blower (just until its colour became grey due to oxidization) before the TEM measurements. The size of a representative nanorod and its electron diffraction pattern are shown in Fig. 3(a) and its inset, respectively. Figure 3(b) clearly shows the atomic layers (200) perpendicular to nanorod axis. A thin amorphous layer of oxidized tin is displayed on the surface of the nanorods, which was resulted from partial oxidization.

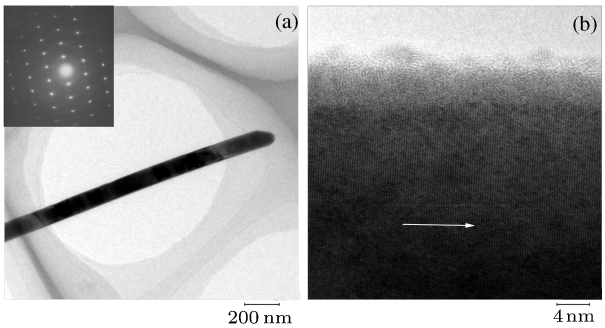


Fig. 3. TEM images of individual nanorods from sample Sn-A: (a) an intermediate-magnification image along with the electron diffraction pattern shown in the inset taken along the ⟨010⟩ zone axis, (b) a high-magnification image. The rod axis, indicated by the arrow, is aligned along ⟨200⟩.

It is well known that GLAD produces in principle oblique amorphous nanorods on static substrate. Thus, as is expected, here it must be the baking of the high-temperature evaporator that made the tin nanorods re-crystallized and reoriented. To confirm this point, copper nanorods were grown, for comparison, under the same condition except the higher evaporation temperature. Their SEM images clearly show that the Cu nanorods are of irregular shape and are oblique. The baking did not re-crystallize or reorient the copper nanorods because copper has a much higher melting point. Therefore, from this comparison we can conclude that the baking of the evaporator causes the recrystallization and reorientation of tin nanorods.

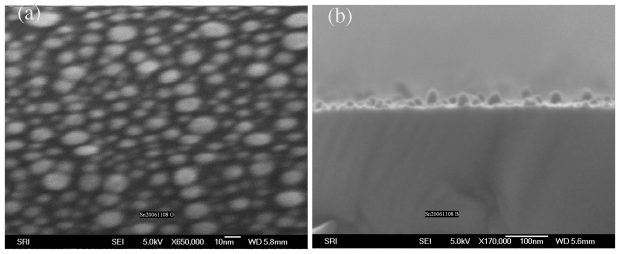


Fig. 4. Top-view (a) and cross-sectional (b) SEM images of tin nano-columnar film in thickness of about 40 nm.

To find out where the recrystallization started from and where it was ongoing (at the top or at the root of a single crystalline nanorod), thinner nano-columnar tin films were grown under lower temperatures by reducing the growth/baking time. When the thickness of the film was about 35 nm (sample Sn-C), tin nanorods show a 'mound' shape and adhesional wetting on the silicon wafer, as shown in Fig. 4. The tin nano-mounds are not of regular shape of single crystal. From larger top-view SEM images (not shown here), few sporadic tin nanorods with regular shape can also be found, indicating that the recrystallization just started at this thickness and corresponding baking time (16.5 min) due to the accumulated temperature resulting from baking. Using an extended growth time to grow a thicker sample (for example, sample Sn-B), we can find that the nanorods were already monocrystalline due to longer baking duration.

Now we can compose a picture of the tin nanorod growth. At the beginning of growth, GLAD produced randomly distributed nano-mounds. As the nano-mounds grew, their temperature increased due to the accumulated baking, so the nano-mounds started to recrystallize at their tops and mono-crystal seeds formed. Atoms of the nano-mounds migrated to the tip of the nano-crystals by surface diffusion and nucleated there until they were used up. Simultaneously, the newly arriving Sn atoms landed on the top parts of the already grown nanorods due to shadowing effect and immediately migrated to the tips of the nano-crystals. Therefore, when the temperature of the sample was increased close to the melting point of tin nanocrystal, the growth process is mainly controlled by high surface mobility of tin atoms.

The tin nanorods can be transferred to SnO_2 nanorods,[11] as partially exemplified by the heated sample Sn-A shown in Fig. 3(b). This route is an easily generalizable strategy for topotactically converting metal nanowires to their oxides as a structure-preserving oxidation process.

In summary, strong surface diffusion mediated glancing-angle deposition method has been used to grow tin nanorods via thermal evaporation technique. Due to the baking of the hot evaporator, the amorphous or polycrystalline tin nanorods start to recrystallize about 16 min after the growth and baking began. The recrystallization continues at high temperature and the resulted monocrystalline tin nanorods prefer to orienting along the surface normal around which the direction of the nanorods distributes in a large angle range. High surface mobility of tin adatoms is thought of as the main driving force for the recrystallization of the GLAD nanorods.

References

[1] Peng X and Chen A 2005 *Appl. Phys. A: Mat. Sci. Proc.* **80** 473
[2] Kayes B M, Atwater HA and Lewis N S 2005 *J. Appl. Phys.* **97** 14302
[3] Robbie K and Brett M J 1997 *J. Vac. Sci. Technol.* A **15** 1460
[4] Zhao Y P et al 2002 *Intl. J. Nanosci.* **1** 87
[5] Wang H H and Zhao Y P 2006 *J. Vac. Sci. Techol.* B **24** 1230
[6] Harris K D, Vick D, Smy T and Brett M J 2002 *J. Vac. Sci. Technol.* A **20** 2062
[7] Zhao Y Pet al 2002 *Nano Lett.* **2** 351
[8] Schubert E et al 2006 *J. Appl. Phys.* **100** 016107
[9] Suzuki M et al 2001 *Appl. Phys. Lett.* **78** 3968
[10] Takeda Y et al 2006 *Conference Record of the 2006 IEEE 4th World Conference on Photovoltaic Energy Conversion* **1/2** 75
[11] Kolmakov A et al 2003 *Nano Lett.* **3** 1125